Available online at www.sciencedirect.com

ScienceDirect

Ceramics International 40 (2014) 3571–3577

CERAMICS INTERNATIONAL

www.elsevier.com/locate/ceramint

Magnetic, ferromagnetic resonance and electrical transport study of $Ni_{1-x}Tb_xFe_2O_4$ spinel ferrites

Muhammad Azhar Khan[a,*], Misbah ul Islam[b], M. Asif Iqbal[b], Mukhtar Ahmad[b], Muhammad F. Din[b], G. Murtaza[c], Ishtiaq Ahmad[b], Muhammad Farooq Warsi[d]

[a]Department of Physics, The Islamia University of Bahawalpur, Bahawalpur 63100, Pakistan
[b]Department of Physics, Bahauddin Zakariya University, Multan 60800, Pakistan
[c]Centre for Advanced Studies in Physics, G.C. University, Lahore 54000, Pakistan
[d]Department of Chemistry, The Islamia University of Bahawalpur, Bahawalpur 63100, Pakistan

Received 30 August 2013; received in revised form 16 September 2013; accepted 16 September 2013
Available online 21 September 2013

Abstract

The impacts of terbium (Tb) contents on magnetic, ferromagnetic resonance (FMR), electrical and dielectric properties of $Ni_{1-x}Tb_xFe_2O_4$ ferrites were investigated. A vibrating sample magnetometer was employed to probe the magnetic properties of the samples at room temperature. It was found that with the increased terbium content, the coercive force and saturation magnetization were decreased which may be attributed to spin canting. Magnetic dynamics of the samples were studied by ferromagnetic resonance in X band (9.5 GHz) at room temperature. The incorporation of terbium sufficiently lowers the FMR line-width. The decrease in FMR line-width is attributed to the reduction of super-exchange interactions. The DC electrical resistivity and activation energy are higher for the substituted samples. The dielectric constant, dielectric loss ($\tan\delta$) and AC-conductivity decreased on account of doping. The decrease in dielectric constant is imputed to the reduction in the internal viscosity of the doped samples. The dielectric data are explained on the basis of space charge polarization. As Ni–Tb ferrites have low value of coercivity, high dielectric constant and low $\tan\delta$, they may be attractive for application in switching and memory storage devices.

Keywords: C. Electrical properties; Ferromagnetic resonance; Magnetic measurements; Ni–Tb ferrites

1. Introduction

The substituted ferrites with the spinel structure have been extensively studied due to their considerable importance to the electronic materials industry. The spinel ferrites are technologically important class of magnetic oxides due to their magnetic properties, high electrical resistivity and low dielectric loss. These properties of spinel ferrites strongly depend on their chemical composition, cation distribution, method of preparation in general and structure in particular. Many efforts have been made to improve the basic properties of spinel ferrites by substituting various ions with different valence states [1]. Nickel ferrite ($NiFe_2O_4$) has been the subject of extensive investigations since past few decades, due to their unique electrical and magnetic behaviors that lead to their widespread technological applications. These materials are used in magnetic drug delivery, transformer core, microwave devices, magnetic information storage media, read/write heads for digital tapes and switching applications [2,3]. Rare-earth substituted nickel spinel ferrites have attracted great attention in the field of materials science owing to their enhanced magnetic and electrical properties [4–6]. The rare-earth ions are promising substitutes for the improvement of the properties of spinel ferrites. The rare-earth elements have unpaired 4f electrons and strong spin–orbit coupling of the angular momentum. The 4f shell of rare-earth elements is shielded by $5s^25p^6$ and almost not affected by the potential field of surrounding ions. The substitution of rare-earth ions into spinel ferrites and the occurrence of 4f–3d couplings in ferrites can improve the magnetic and electrical transport properties of $NiFe_2O_4$ ferrites.

Ferromagnetic resonance (FMR) is an important tool to study the magnetic dynamical properties of spinel ferrites. The

*Corresponding author. Tel.: +92 62 9255461; fax: +92 62 9255474.
E-mail address: azhar_manais@hotmail.com (M.A. Khan).

0272-8842/$ - see front matter © 2013 Elsevier Ltd and Techna Group S.r.l. All rights reserved.
http://dx.doi.org/10.1016/j.ceramint.2013.09.071

information regarding the homogeneity and magnetization relaxation behavior can be determined from FMR positions and linewidths (ΔH) of the ferrite materials. FMR spectra of the Ni–Zn–Cr ferrites have been reported. It was observed that the $Ni_{0.5}Zn_{0.5}Fe_2O_4$ and $Ni_{0.5}Zn_{0.5}Fe_{1.9}Cr_{0.1}O_4$ compositions exhibit large values (1139 Oe and 1165 Oe respectively) of FMR line-width (ΔH) [7–9].

Studies concerning the effects of substitution of Tb, Dy, Yb, Er, Gd, Sm, Ce, Y, Eu, La, Th, etc., in various spinel ferrites have been carried out by several researchers [10–12]. The purpose of the investigation is to study the effect of terbium ions substitution for nickel ions on magnetic, ferromagnetic, electrical and dielectric properties of $Ni_{1-x}Tb_xFe_2O_4$ ferrites to make these ferrites suitable for switching and memory storage devices applications.

2. Experimental procedure

The experimental details of sample preparation that were followed are already reported elsewhere [13]. The *hysteresis loops* were recorded at room temperature on a computer controlled vibrating sample magnetometer (VSM), LakeShore model 7300. The ferromagnetic resonance (FMR) measurements were performed on spherical shaped samples using a standard FMR spectrometer at X-band (9.5 GHz) in a TE_{102} reflection cavity. The measurements were made under identical conditions on all the samples. In FMR measurements, the sample was always saturated due to a static magnetic field required for resonance at microwave frequency. The DC resistivity of all the samples at different temperatures was measured by the two probe method in the temperature range 303–473 K. An impedance analyzer along with a specifically tuned cell was used to study dielectric properties for $Ni_{1-x}Tb_xFe_2O_4$ ferrites. The dielectric constant (ε') and dielectric loss ($\tan\delta$) were measured in the frequency range from 10 Hz to 10 MHz. The dielectric constant for the samples was calculated by using the following equation:

$$\varepsilon = \frac{Cd}{\varepsilon_o A} \quad (1)$$

In Eq. 1, C is the capacitance in Farad and d is the thickness of pellet in meters; A is the cross sectional area of the flat surface of the pellet and ε_o is the permittivity of free space. The AC electrical conductivity of all the samples was calculated using the following equation:

$$\sigma_{AC} = 2\pi(\tan\ \delta)\varepsilon'\varepsilon_o \quad (2)$$

In Eq. 2 above, $\tan\delta$ is the dissipation factor.

3. Results and discussion

3.1. Magnetic properties

The hysteresis loops of $Ni_{1-x}Tb_xFe_2O_4$ ferrites are shown in Fig. 1. The narrow magnetic hysteresis loops of the samples indicate that the samples are magnetically soft, with low coercivity. All the loops behaved normally, and the magnetization

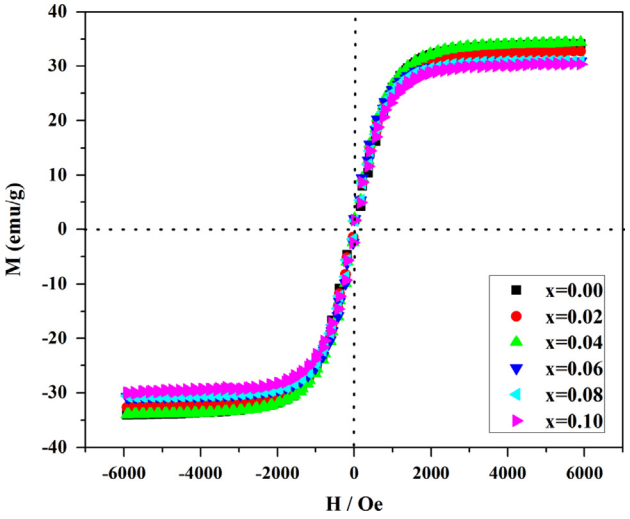

Fig. 1. Hysteresis loops for $Ni_{1-x}Tb_xFe_2O_4$ (x=0, 0.02, 0.04, 0.06, 0.08, and 0.10) ferrites.

Table 1
Magnetic data on $Ni_{1-x}Tb_xFe_2O_4$ ferrites.

Sl. no.	Composition	M_s (emu g^{-1})	H_c (Oe)
1	$NiFe_2O_4$	34.05	40.00
2	$Ni_{0.98}Tb_{0.02}Fe_2O_4$	34.16	35.00
3	$Ni_{0.96}Tb_{0.04}Fe_2O_4$	32.70	30.00
4	$Ni_{0.94}Tb_{0.06}Fe_2O_4$	30.82	29.50
5	$Ni_{0.92}Tb_{0.08}Fe_2O_4$	30.72	29.00
6	$Ni_{0.90}Tb_{0.10}Fe_2O_4$	30.20	27.50

increased with increasing applied magnetic field. Various magnetic parameters such as saturation magnetization (M_s) and coercivity (H_c) were obtained from the hysteresis loops for the Tb substituted nickel ferrites and are compared with those of un-substituted nickel ferrites (Table 1) [14–16]. A decrease in saturation magnetization has been observed with the substitution of terbium. This decrease may be attributed to the weakening of A–B interactions. There are three types of negative exchange interactions [17] between the unpaired electrons of two ions lying in A- and B-sites. The A–B interaction heavily predominates over A–A and B–B interactions. The net magnetic moment of the whole lattice is the difference between the moments of the B- and A-sublattices, i.e. $M=|M_B-M_A|$, where M_A and M_B are the magnetic moments of the A and B sites respectively. It is an established fact that $NiFe_2O_4$ ferrite adopts an inverse spinel structure. In nickel ferrite, most of the Ni^{2+} ions occupy octahedral sites (B-sites) and the Fe^{3+} ions are distributed on both octahedral and tetrahedral sites (A-sites) [18,19]. The magnetic moment at each composition depends on the magnetic moments of the constituent ions involved. The magnetic moments of Fe^{3+} and Ni^{2+} are 5 μ_B and 2 μ_B respectively while terbium is paramagnetic. The substitution of Tb (0.93 Å) with Ni (0.69 Å) ions takes place on octahedral sites due to larger ionic radius and the possibility of occupying tetrahedral sites is rare as reported in our previous work [13]. Therefore, it is expected that the

number of magnetic moments on the octahedral sites will decrease. Thus the magnetic moment of B-sublattice decreases and consequently the net magnetization is decreased. In the present investigation the decrease of magnetization with Tb contents is consistent with results reported by other researchers [20–22]. A slight increase in saturation magnetization for x=0.02 may be due to the migration of a few Fe^{3+} ions on the B-sites from A-sites. The coercivity is observed to decrease as the concentration of terbium is increased. Due to smaller values of coercivity these materials can be used in the switching devices.

3.2. Ferromagnetic resonance (FMR) studies

Various FMR parameters such as FMR linewidth (ΔH), FMR position (H) and FMR intensity (I) were calculated from the FMR profiles of the synthesized materials which were recorded using an X-band (9.5 GHz) FMR spectrometer. FMR profiles of $Ni_{1-x}Tb_xFe_2O_4$ (x=0, 0.02, 0.04, 0.06, 0.08, and 0.10) ferrites measured at X-band (9.5 GHz) are presented in Fig. 2. All the samples under investigation exhibited a single resonance peak and the profiles are slightly asymmetric. The asymmetry may be attributed to the contribution of non-uniform resonance modes apart from the main mode (uniform mode k=0) of resonance. The FMR profiles are seen to broaden which may be due to the decrease in magnetization and Ni^{2+} ions in the samples [23,24]. The FMR line-width depends on the size and surface roughness of the spherical samples [25]. However the variation of the FMR line-width with Tb concentration (Fig. 3) is not due to these factors because the samples are of the same size and have the same surface roughness. The substitution of Tb lowers the FMR line-width from 1180 to 593 Oe up to dopant concentration of x=0–0.6 and then increases at higher dopant contents. The behavior of FMR line-width is more or less similar to that of the saturation magnetization. The variations of FMR line-widths and FMR position with Tb contents are shown in Fig. 3. The minimum relaxation time calculated from FMR line-widths for these ferrites is $\sim 10^{-10}$ s. The substitution of Tb in $NiFe_2O_4$ greatly influences the intensities of the FMR

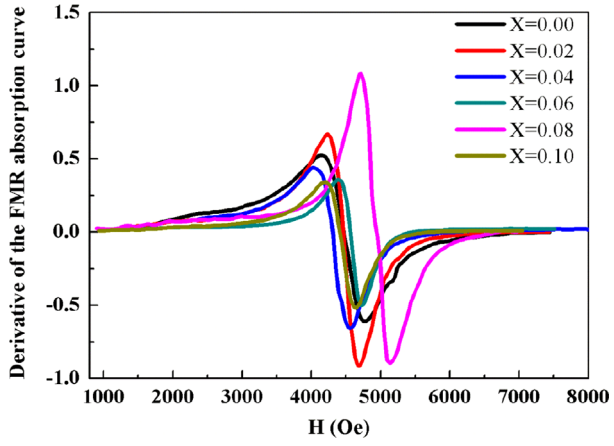

Fig. 2. Room temperature FMR profiles for $Ni_{1-x}Tb_xFe_2O_4$ (x=0, 0.02, 0.04, 0.06, 0.08, and 0.10) ferrites taken at X-band (9.5 GHz).

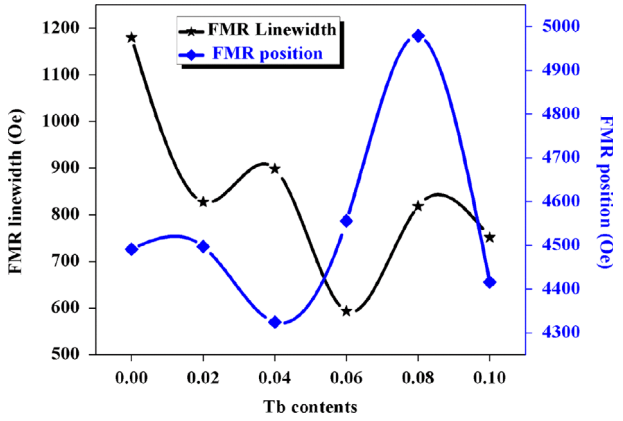

Fig. 3. Variation of FMR linewidth and FMR position for $Ni_{1-x}Tb_xFe_2O_4$ (x=0, 0.02, 0.04, 0.06, 0.08, and 0.10) ferrites taken at X-band (9.5 GHz).

profiles (Fig. 2). FMR intensities of the profiles depend on the gyromagnetic ratio (γ), morphology and g-values of the different cations. The gyromagnetic ratio (γ) has different values for nickel, ferric and terbium ions because of the differences in the spectroscopic splitting g-factors. The g-values for Ni^{2+} lie in the range 2.15–2.35 and for Fe^{3+} g=2. The g-value for terbium ions is $\sim$1.95 [26]. The above mentioned differences in the g-values of the cations involved are responsible for the observed variations in the intensity of the FMR profiles. The highest intensity observed for sample x=0.08 could be attributed to the formation of agglomerates [27].

3.3. DC electrical resistivity

Room temperature DC resistivity of $Ni_{1-x}Tb_xFe_2O_4$ ferrites was measured by the two probe method. It has been noticed that the resistivity increased linearly from 1.7×10^5 Ω cm to 2.8×10^5 Ω cm as the concentration of terbium was increased from 0.0 to 0.1 in steps of 0.02. The increase in resistivity is associated with the larger ionic radius of Tb^{3+} (0.93 Å) as compared to the Ni^{2+} (0.69 Å) which could cause strain in the spinel lattice and obscure the conduction process in these ferrites. These results are consistent with the reported results for similar compounds [10,28]. The increase in resistivity may be also due to 4f–3d coupling between transition metal nickel and rare earth terbium ions.

Temperature dependent electrical resistivity was measured in the temperature range of 303–473 K (Fig. 4). The resistivity decreased with the increased temperature (Arrhenius equation) [29]:

$$\rho = \rho_o e^{\frac{Ea}{k_B T}} \tag{3}$$

In the above equation, ρ_0 is a constant, E_a is the activation energy, k_B is Boltzmann's constant and T is the absolute temperature. The resistivity decreases as temperature increases that indicates the semiconducting behavior of the samples [30]. The drift mobility was calculated from the electrical resistivity data using the following equation [31]:

$$\mu_d = \frac{1}{ne\rho} \tag{4}$$

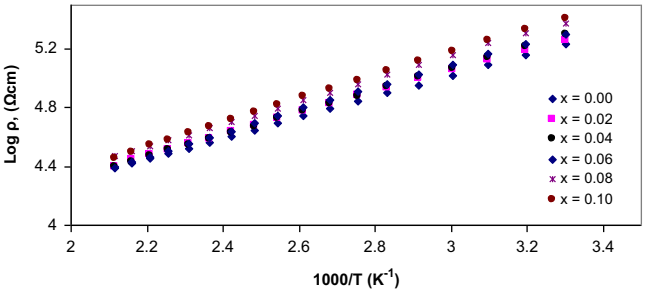

Fig. 4. Variation of DC electrical resistivity (log ρ) with temperature (1000/T) for $Ni_{1-x}Tb_xFe_2O_4$ spinel ferrites.

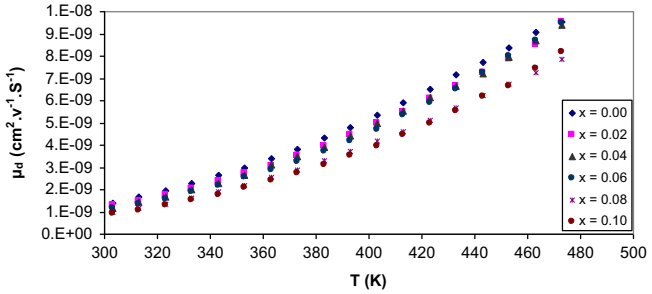

Fig. 5. Drift mobility (μ_d) as a function of temperature (1000/T) for $Ni_{1-x}Tb_xFe_2O_4$ spinel ferrites.

In Eq. 4, e is the charge of electron, ρ is the electrical resistivity and n is the concentration of charge carriers. The value of charge carriers i.e. n was determined by the following relation:

$$n = \frac{N_A C_{Fe} \rho_b}{M} \quad (5)$$

where N_A is Avogadro's number, C_{Fe} is the number of iron atoms in the chemical formula of the samples, ρ_b is the bulk density and M is the molar mass of the sample. The variation of drift mobility with temperature is shown in Fig. 5. It can be seen that as temperature increases the drift mobility also increases. This is due to the hopping of charge carriers between similar lattice sites. The drift mobility at room temperature decreases from 1.4×10^{-9} to 0.9×10^{-9} $cm^2 V^{-1} s^{-1}$ on increasing the terbium concentration from 0.0 to 0.1. The conduction mechanism [32] in nickel ferrites is due to both n- and p-type charge carriers. The n-type charge carriers are electrons hopping between iron ions and p-type carriers are holes hopping between the nickel ions at the octahedral sites. The following conduction mechanism in these ferrites can be proposed:

$$Fe^{2+} \leftrightarrow Fe^{3+} + e^- \quad (6)$$

$$Ni^{3+} + e^- \leftrightarrow Ni^{2+} \quad (7)$$

By combining Relations 6 and 7, the following relation is obtained:

$$Fe^{3+} + Ni^{2+} \leftrightarrow Fe^{2+} + Ni^{3+} \quad (8)$$

The increase in resistivity is associated with the distribution of cations on the sublattices. When terbium is substituted for Ni ions, it is expected to occupy the octahedral sites because nickel ferrite has an inverse spinel structure [33] in which nickel ions occupy the octahedral sites. The number of Ni^{2+} and Ni^{3+} ions on the octahedral sites will be decreased. The resistivities of the samples depend on the hopping probability of both types of charge carriers. Therefore, the incorporation of terbium ions at the cost of nickel ions causes the increase in resistivity. The presence of terbium ions on the octahedral sites and on the grain boundaries hampers the degree of easy conduction between the nickel and iron ions on the octahedral sites, thereby increasing the resistivity of the samples under investigation. Increase in resistivity was reported [34] when gadolinium was substituted in nickel ferrites. The activation energy derived from Arrhenius plots varies with the terbium contents in a similar manner to that of the room temperature DC electrical resistivity. It can be inferred that the samples that have high resistivity have high activation energy and vice versa. The activation energy values for the present system range from 0.14 to 0.16 eV and are in accordance with Verwey's hopping conduction mechanism.

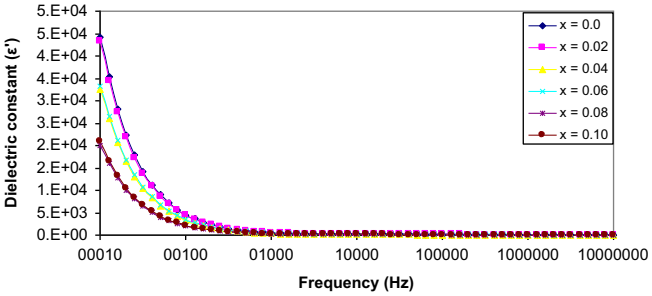

Fig. 6. Dielectric constant (ε') as a function of frequency for $Ni_{1-x}Tb_xFe_2O_4$ spinel ferrites.

3.4. Dielectric properties

The frequency and composition dependent dielectric constant (ε') for $Ni_{1-x}Tb_xFe_2O_4$ spinel ferrites was measured in the frequency range 10 Hz–10 MHz. The variation of dielectric constant (ε') with frequency at room temperature for all the samples under investigation is shown in Fig. 6 and it revealed that the dielectric constant decreases continuously with increase in frequency. The dielectric constant is almost frequency independent at high frequency. This indicates that the dispersion is due to Maxwell–Wagner type interfacial polarization which is in good agreement with Koop's phenomenological theory. According to these models, the dielectric structure consists of two layers. The first layer, which is composed of ferrite grains, is a well conducting material and it is separated by a thin layer of poorly conducting material called grain boundaries [34]. The observed frequency independent behavior is due to the fact that the electric dipoles are unable to follow the fast variation of the alternating applied electric field at very high frequencies [35].

It has been noticed that the dielectric constant decreases with the substitution of terbium. The decrease in the values of dielectric constant with dopant concentration may be attributed to the decrease in internal viscosity of the system which

provides more degrees of freedom to the dipoles of the system, contributing to polarization. Thus disordering increases in the system and hence the dielectric constant decreases. The hopping of electrons from Fe^{3+} to Fe^{2+} ions and hole hopping between Ni^{3+} and Ni^{2+} ions at B-sites are responsible for the polarization in these ferrites. The hopping between A-sites is rare as there are only Fe^{3+} ions present on A-sites and Fe^{2+} ions which are formed in the course of processing occupy only B-sites [36]. As a result of the substitution of terbium for the Ni ions, the Ni as well as Fe ions on B-sites may decrease in number ($Fe^{3+}+Ni^{2+}\leftrightarrow Fe^{2+}+Ni^{3+}$). Therefore the dielectric polarization in the external applied field decreases. This explains the reason for the decrease of the dielectric constant due to the terbium substitution.

It has been noticed that there is no dispersion in the dielectric constant (ε') of all the samples in the studied frequency range. All samples show high dielectric constant on the order of 10^3–10^4 at very low frequencies. The higher values of dielectric constant in the lower frequency region are explained on the basis of space charge polarization. This type of polarization is attributed to the heterogeneity of the samples and to the fact that ferroelectric regions are surrounded by non-ferroelectric regions similar to the case of relaxor ferroelectric materials [37].

Fig. 7 shows the variation of dielectric loss ($\tan\delta$) with frequency for $Ni_{1-x}Tb_xFe_2O_4$ spinel ferrites. The relations of $\tan\delta$ with frequency in the MHz range show a relaxation spectrum with a loss peak. It has been reported [38] that the occurrence of loss peak in the $\tan\delta$ versus frequency is associated with the strong correlation between the hopping conduction mechanism and dielectric behavior of spinel ferrites (i.e. the cation–cation correlation at the octahedral site). The appearance of loss peak in $\tan\delta$ is known as abnormal dielectric loss and it has been observed for all the samples which could be related to the resonance effect. The dielectric loss in ferrites is the result of lagging of polarization ions with respect to the applied alternating electric field. This abnormal behavior may be also attributed to the presence of both types of charge carriers [39]. In Ni ferrites the conduction mechanism is p-type due to the hole exchange between Ni^{3+} and Ni^{2+}. The electrons initiated from the hopping process between $Fe^{2+}\leftrightarrow Fe^{3+}+e^-$ capture some Ni^{3+} ions and it results in the formation of Ni^{2+} ions. With the substitution of terbium, in place of nickel, the loss peaks become broader. It is

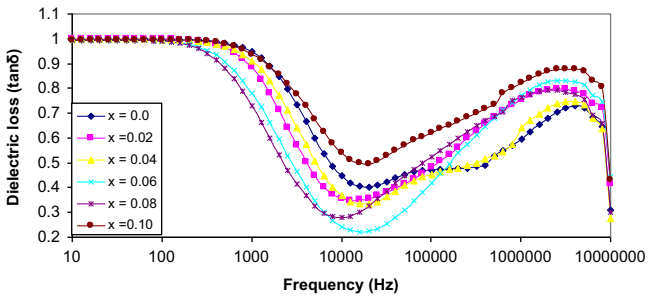

Fig. 7. Dielectric loss ($\tan\delta$) as a function of frequency for $Ni_{1-x}Tb_xFe_2O_4$ spinel ferrites.

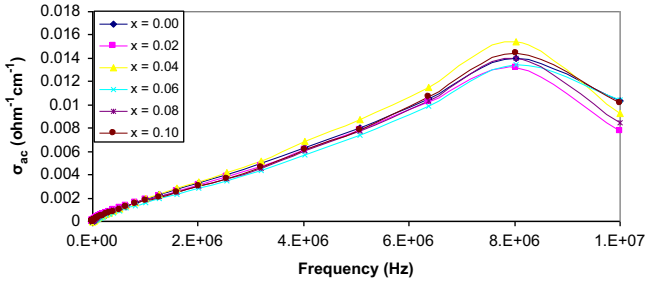

Fig. 8. AC conductivity as a function of frequency for $Ni_{1-x}Tb_xFe_2O_4$ spinel ferrites.

worth noticing that the dielectric loss increases with the increase of Tb contents. The increase in the dielectric loss could be attributed to the cluster formation and this acts as the trapping centers at different depths. Similar kinds of abnormal dielectric loss behavior have been reported for Mn–Zn ferrites [39]. It has been observed that the values of the dielectric loss are less than 1 even in the MHz frequency range and these values are significantly lower compared to the ferrites synthesized by conventional method [40].

The variation of AC conductivity with frequency for $Ni_{1-x}Tb_xFe_2O_4$ ferrites at room temperature is shown in Fig. 8. The total AC conductivity of ferrites is given by the following relation:

$$\sigma_{tot}=\sigma_1(T)+\sigma_2(\omega,T) \quad (9)$$

The first term σ_1 indicates the DC conductivity. The second term is frequency dependent and it actually exhibits AC conductivity due to electron hopping amongst the sites. In all the samples it has been observed that the AC conductivity gradually increases as the frequency of the applied external field increases. An increase in frequency increases the electron hopping frequency of the charge carriers; hence the conductivity increases. The electron hopping and liberated charge together provide the basis for the conduction mechanism in ferrites. The AC conductivity generally decreases by the Tb-substitution. This may be due to the inclusion of Tb-ions in the spinel lattice which affects the conduction mechanism. The sample $x=0.04$ exhibits high conductivity in the high frequency region in comparison to the neighboring compositions and there is an anomaly in this behavior. A decrease in the conductivity of all the samples is noted beyond 8 MHz and this can be attributed to the occurrence of loss peaks appearing in the dielectric loss.

4. Conclusions

The substitution of terbium in nickel ferrites caused the decrease of saturation from 34 to 30 emu g^{-1}. The coercivity decreases from 40 to 27.5 Oe as the concentration of terbium is varied from 0 to 0.1. The substituted samples exhibit smaller values of FMR line-widths and have better correlation with the saturation magnetization. The sample $Ni_{0.94}Tb_{0.06}Fe_2O_4$ has minimum FMR line-width ($\Delta H=593$ Oe), which is minimum as compared to the reported line-widths for spinel ferrites. The DC electrical resistivity and activation energy were found to

increase by the increase in dopants concentration. The drift mobility decreases from 1.4×10^{-9} to 0.97×10^{-9} $cm^2 V^{-1} s^{-1}$ on increasing the terbium concentration. The decrease in the values of dielectric constant by the introduction of terbium in these ferrites is attributed to the decrease in the internal viscosity of the system which contributes to the polarization. The appearance of loss peak in the dielectric loss indicates a strong correlation between the hopping conduction mechanism and the dielectric behavior of these ferrites. The reduced coercive force, high dielectric constant and smaller dielectric loss of $Ni_{1-x}Tb_xFe_2O_4$ ferrites suggest their utility in the fabrication of switching and memory storage devices.

Acknowledgments

The authors acknowledge the financial support of Higher Education Commission (HEC) of Pakistan under Indigenous Ph.D. Fellowship Scheme and Project no. PD-IPFP/HRD/HEC/2013/1912.

References

[1] J. Smit, H.P.J. Wijn, Ferrites, Philips Technical Library, Eindhoven, Netherlands278–282.
[2] I. Maghsoudi, H. Shokrollahi, M.J. Hadianfard, J. Amighian, Synthesis and characterization of $NiAl_xFe_{2-x}O_4$ magnetic spinel ferrites produced by conventional method, Powder Technology 235 (0) (2013) 110–114.
[3] M.N. Ashiq, M.F. Ehsan, M.J. Iqbal, I.H. Gul, Synthesis, structural and electrical characterization of Sb^{3+} substituted spinel nickel ferrite ($NiSb_xFe_{2-x}O_4$) nanoparticles by reverse micelle technique, Journal of Alloys and Compounds 509 (16) (2011) 5119–5126.
[4] Y. Zhang, D. Wen, Effect of RE/Ni (RE=Sm, Gd, Eu) addition on the infrared emission properties of Co–Zn ferrites with high emissivity, Materials Science and Engineering B 172 (3) (2010) 331–335.
[5] M. Ishaque, M.U. Islam, M.A. Khan, I.Z. Rahman, A. Genson, S. Hampshire, Structural, electrical and dielectric properties of yttrium substituted nickel ferrites, Physica B: Physics of Condensed Matter 405 (6) (2010) 1532–1540.
[6] E. Melagiriyappa, H.S. Jayanna, Structural and magnetic susceptibility studies of samarium substituted magnesium–zinc ferrites, Journal of Alloys and Compounds 482 (1–2) (2009) 147–150.
[7] H. Montiel, G. Alvarez, M.P. Gutiérrez, R. Zamorano, R. Valenzuela, Microwave absorption in Ni–Zn ferrites through the Curie transition, Journal of Alloys and Compounds 369 (1–2) (2004) 141–143.
[8] L. Gama, E.P. Hernandez, D.R. Cornejo, A.A. Costa, S.M. Rezende, R.H.G.A. Kiminami, A.C.F.M. Costa, Magnetic and structural properties of nanosize Ni–Zn–Cr ferrite particles synthesized by combustion reaction, Journal of Magnetism and Magnetic Materials 317 (1–2) (2007) 29–33.
[9] R. Valenzuela, Magnetic Ceramics, Cambridge University Press, New York, USA, 1994.
[10] M.A. Khan, M.U. Islam, M. Ishaque, I.Z. Rahman, Effect of Tb substitution on structural, magnetic and electrical properties of magnesium ferrites, Ceramics International 37 (7) (2011) 2519–2526.
[11] E. Rezlescu, N. Rezlescu, P.D. Popa, L. Rezlescu, C. Pasnicu, The influence of R_2O_3 (R=Yb, Er, Dy, Tb, Gd, Sm and Ce) on the electric and mechanical properties of a nickel–zinc ferrite, Physica Status Solidi A 162 (2) (1997) 673–678.
[12] M.A. Ahmed, N. Okasha, M.M. El-Sayed, Enhancement of the physical properties of rare-earth-substituted Mn–Zn ferrites prepared by flash method, Ceramics International 33 (1) (2007) 49–58.
[13] M.A. Khan, M.U. Islam, M. Ishaque, I.Z. Rahman, A. Genson, S. Hampshire, Structural and physical properties of Ni–Tb–Fe–O system, Materials Characterization 60 (1) (2009) 73–78.
[14] A.G. Bhosale, B.K. Chougule, X-ray, infrared and magnetic studies of Al-substituted Ni ferrites, Materials Chemistry and Physics 97 (2–3) (2006) 273–276.
[15] S. Singhal, K. Chandra, Cation distribution and magnetic properties in chromium-substituted nickel ferrites prepared using aerosol route, Journal of Solid State Chemistry 180 (1) (2007) 296–300.
[16] K. Maaz, W. Khalid, A. Mumtaz, S.K. Hasanain, J. Liu, J.L. Duan, Magnetic characterization of $Co_{1-x}Ni_xFe_2O_4$ ($0 \leq \times x \leq 1$) nanoparticles prepared by co-precipitation route, Physica E: Low-dimensional Systems and Nanostructures 41 (4) (2009) 593–599.
[17] I. Neel, Propriétés magnétiques des ferrites. Ferrimagnétisme et antiferromagnétisme, Annals of Physics 3 (1948) 137–198.
[18] C.N. Chinnasamy, A. Narayanasamy, N. Ponpandian, K. Chattopadhyay, K. Shinoda, B. Jeyadevan, K. Tohji, K. Nakatsuka, T. Furubayashi, I. Nakatani, Mixed spinel structure in nanocrystalline $NiFe_2O_4$, Physical Review B 63 (18) (2001) 184108.
[19] H. Perron, T. Mellier, C. Domain, J. Roques, E. Simoni, R. Drot, H. Catalette, Structural investigation and electronic properties of the nickel ferrite $NiFe_2O_4$: a periodic density functional theory approach, Journal of Physics: Condensed Matter 19 (2007) 346219.
[20] N. Rezlescu, E. Rezlescu, C. Pasnicu, M.L. Craus, Effects of the rare-earth ions on some properties of a nickel–zinc ferrite, Journal of Physics: Condensed Matter 6 (1994) 5707–5716.
[21] E. Rezlescu, N. Rezlescu, C. Pasnicu, M.L. Craus, P.D. Popa, Effects of rare-earth ions on the quality of a Li–Zn ferrite, Crystal Research and Technology 31 (3) (1996) 343–352.
[22] N. Rezlescu, E. Rezlescu, The influence of Fe substitutions by R ions in a Ni–Zn ferrite, Solid State Communications 88 (2) (1993) 139–141.
[23] D. Jiles, Introduction to Magnetism and Magnetic Materials, Chapman & Hall, London, UK, 1991.
[24] B.P. Rao, O.F. Caltun, Synthesis and characterization of some ferrite nanoparticles, Journal of Optoelectronics and Advanced Materials 8 (2006) 991–994.
[25] G.F. Dionne, Effect of surface roughness on ferrimagnetic resonance linewidth measurements, Journal of Applied Physics 43 (3) (1972) 1221–1224.
[26] B.P. Rao, A.M. Kumar, K.H. Rao, Y.L.N. Murthy, O.F. Caltun, I. Dumitru, L. Spinu, Synthesis and magnetic studies of Ni–Zn ferrite nanoparticles, Journal of Optoelectronics and Advanced Materials 8 (2006) 1703–1705.
[27] N. Guskos, G. Zolnierkiewicz, J. Typek, D. Sibera, U. Narkiewicz, Magnetic resonance study of $ZnO–Fe_2O_3$-$ZnFe_2O_4$ system, Reviews on Advanced Materials Science 23 (2010) 24–228.
[28] N. Rezlescu, E. Rezlescu, P.D. Popa, L. Rezlescu, Effects of rare-earth oxides on physical properties of Li–Zn ferrite, Journal of Alloys and Compounds 275–277 (0) (1998) 657–659.
[29] K.J. Standley, Oxide Magnetic Materials, Claredon Press, Oxford, UK, 1962.
[30] M.U. Islam, F. Aen, S.B. Niazi, M.A. Khan, M. Ishaque, T. Abbas, M.U. Rana, Electrical transport properties of CoZn ferrite–SiO_2 composites prepared by co-precipitation technique, Materials Chemistry and Physics 109 (2–3) (2008) 482–487.
[31] M.K. Shobana, S. Sankar, V. Rajendran, Characterization of $Co_{0.5}Mn_{0.5}Fe_2O_4$ nanoparticles, Materials Chemistry and Physics 113 (1) (2009) 10–13.
[32] L.J. Berchmans, R.K. Selvan, C.O. Augustin, Evaluation of Mg^{2+}-substituted $NiFe_2O_4$ as a green anode material, Materials Letters 58 (12–13) (2004) 1928–1933.
[33] A.K.M.A. Hossain, S.T. Mahmud, M. Seki, T. Kawai, H. Tabata, Structural, electrical transport, and magnetic properties of $Ni_{1-x}Zn_xFe_2O_4$, Journal of Magnetism and Magnetic Materials 312 (1) (2007) 210–219.
[34] M.Z. Said, Effect of gadolinium substitutions on the structure and electrical conductivity of Ni-ferrite, Materials Letters 34 (3–6) (1998) 305–307.
[35] N. Sivakumar, A. Narayanasamy, B. Jeyadevan, R.J. Joseyphus, Dielectric relaxation behaviour of nanostructured Mn–Zn ferrite, Journal of Physics D: Applied Physics 41 (2008) 245001.
[36] A.M.M. Farea, S. Kumar, K.M. Batoo, A. Yousef, C.G. Lee, Alimuddin, Influence of the doping of Ti^{4+} ions on electrical and magnetic properties of $Mn_{1+x}Fe_{2-2x}Ti_xO_4$ ferrite, Journal of Alloys and Compounds 469 (1–2) (2009) 451–457.

[37] D.C. Agarwal, Asian Journal of Physics 6 (1997) 108–115.
[38] M.K. Fayek, M.K. Elnimr, F. Sayedahmed, S.S. Ata-Allah, M. Kaiser, Relaxation characteristics of $NiGa_xFe_{2-x}O_4$, Solid State Communications 115 (3) (2000) 109–113.
[39] Navneet Singh, Ashish Agarwal, Sujata Sanghi, Satish Khasa, Dielectric loss, conductivity relaxation process and magnetic properties of Mg substituted Ni–Cu ferrites, Journal of Magnetism and Magnetic Materials 324 (2012) 2506–2511.
[40] B.P. Rao, K.H. Rao, Effect of sintering conditions on resistivity and dielectric properties of Ni–Zn ferrites, Journal of Materials Science 32 (22) (1997) 6049–6054.